Morphology, metabolomic and transcriptomic analysis revealed the mechanism of foliar application of triacontanol enhances Cd enrichment in *Tagetes patula* L.

Luqi Mi, Yetong Liu, Qingqing Huang, Lijie Zhao, Xu Qin*, Yuebing Sun*, Boyan Li

Supplementary Material (Figures)

Captions

Fig. S1. Effect of triacontanol on photosynthetic and antioxidant system of *T. patula.*
Fig. S2. Effects of triacontanol on metabolism expression and KEGG enrichment pathway of *T. patula* root.
Fig. S3. The clustering heatmaps of three comparison groups.
Fig. S4. Effects of triacontanols on LMWOA&AAs metabolism in the SP_H_vs_BP_H_vs_CK comparison group.
Fig. S5. Alanine, aspartate, and glutamate metabolism pathway (map00250).
Fig. S6. Effects of triacontanol on gene expression of *T. patula* root.
Fig. S7. Pearson correlation analyses of various leaves parameters.
Fig. S8. Nicotinate, and nicotinamide metabolism pathway (map00760).
Fig. S9. ABC transporters pathway (map02010).

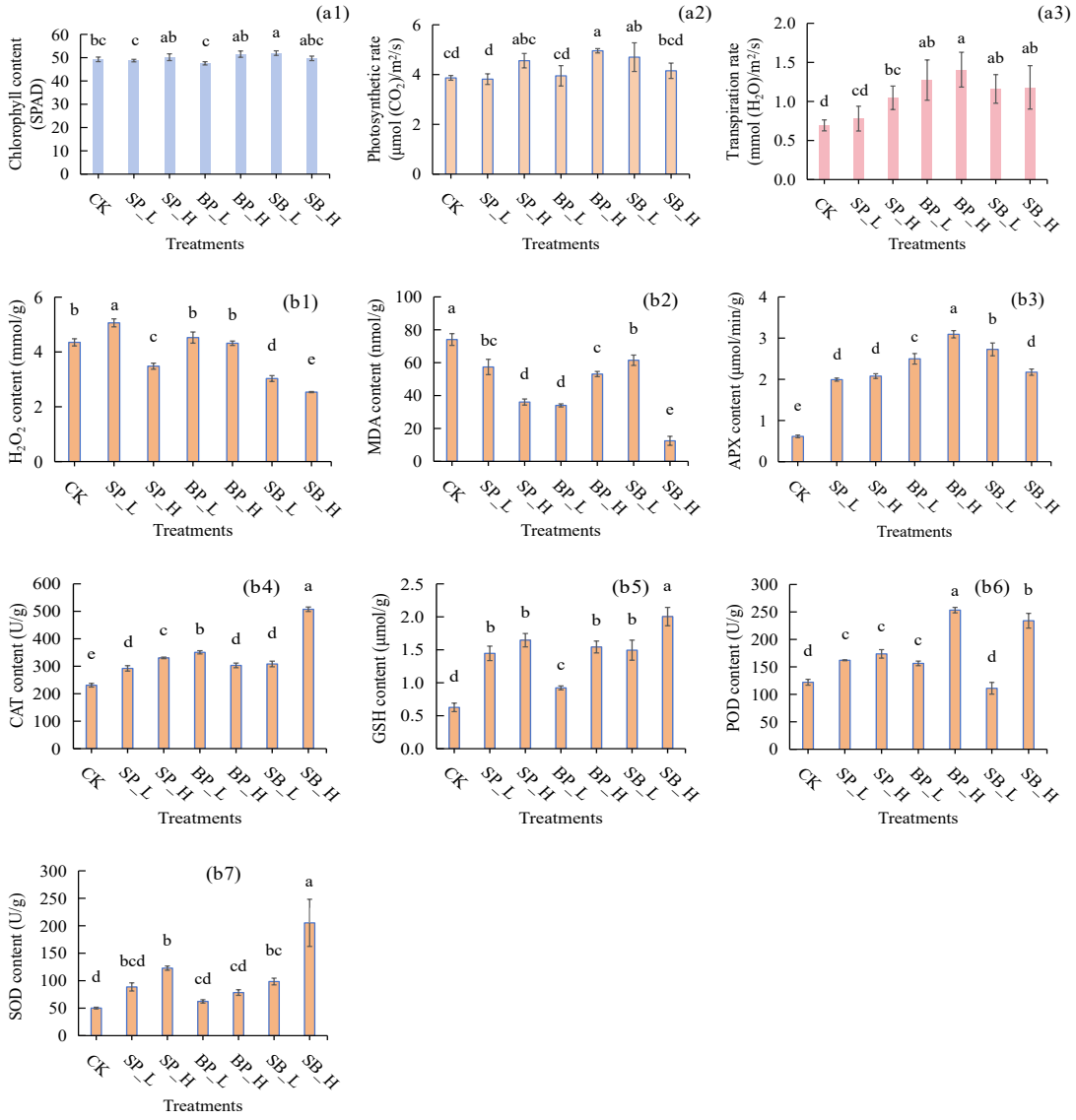

Fig. S1. Effect of triacontanol on photosynthetic (a1-a3) and antioxidant system (b1-b7) of *T. patula.*

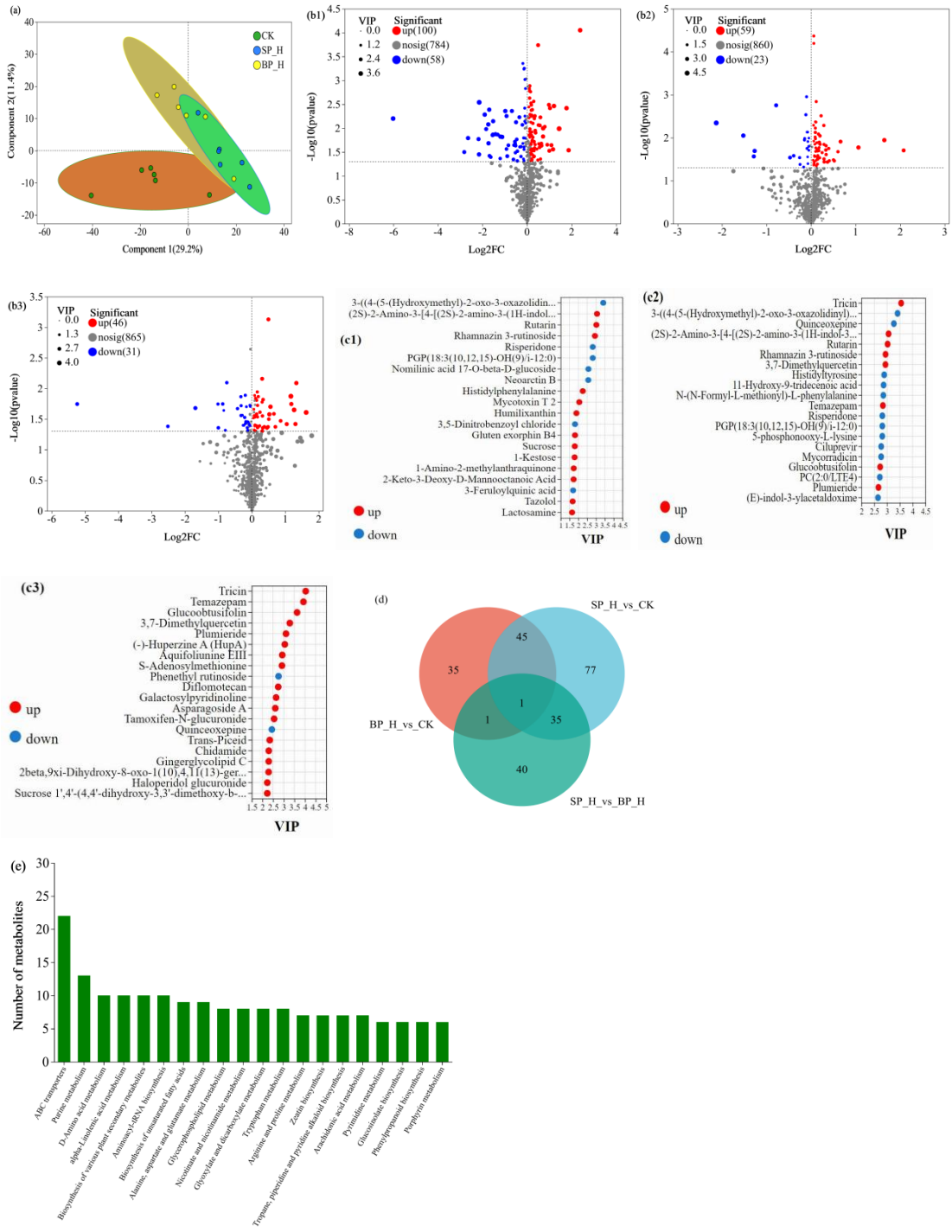

Fig. S2. Effects of triacontanol on metabolism expression and KEGG enrichment pathway of *T. patula* root. (a) Analysis of DEMs based on PLS-DA scores; (b) Volcano plots of upregulated and downregulated DEMs in SP_H_vs_CK (b1), BP_H_vs_CK (b2) and SP_H_vs_BP_H (b3); (c) VIP bar charts of top 20 DEMs in SP_H_vs_CK (c1), BP_H_vs_CK (c2) and SP_H_vs_BP_H (c3); (d) Veen graph between three comparison groups; (e) Top 20 KEGG enrichment pathways.

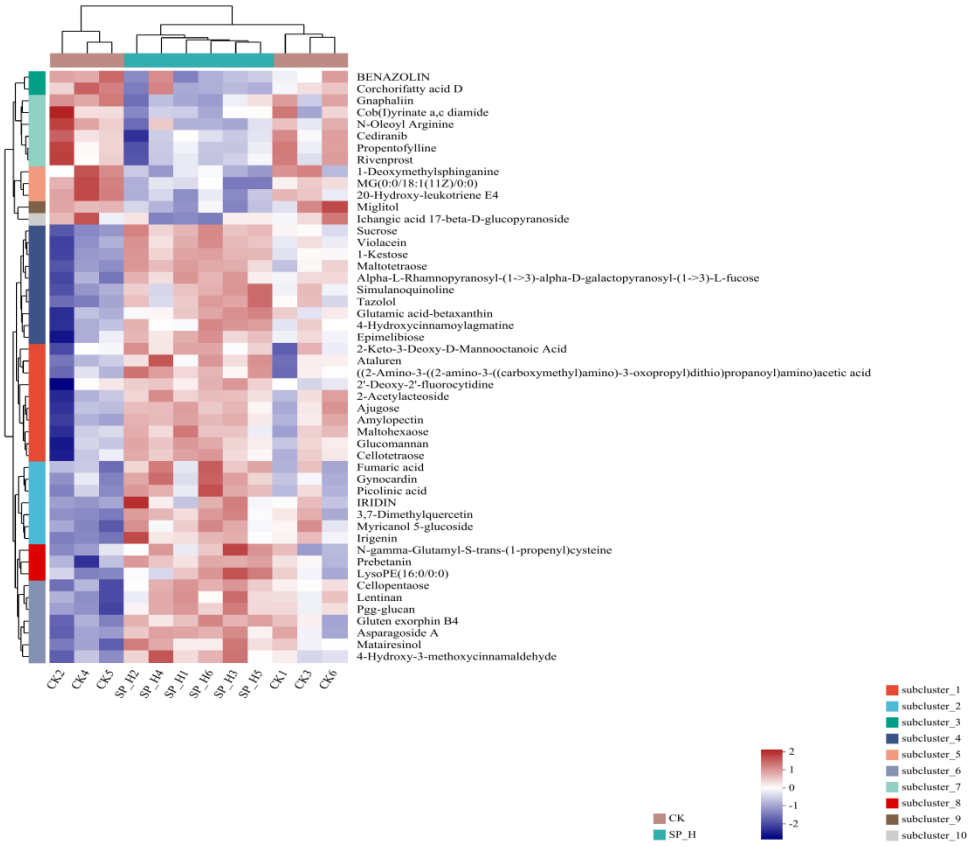
BENAZOLIN
Corchorifatty acid D
Gnaphaliin
Cob(I)yrinate a,c diamide
N-Oleoyl Arginine
Cediranib
Propentofylline
Rivenprost
1-Deoxymethylsphinganine
MG(0:0/18:1(11Z)/0:0)
20-Hydroxy-leukotriene E4
Miglitol
Ichangic acid 17-beta-D-glucopyranoside
Sucrose
Violacein
1-Kestose
Maltotetraose
Alpha-L-Rhamnopyranosyl-(1->3)-alpha-D-galactopyranosyl-(1->3)-L-fucose
Simulanoquinoline
Tazolol
Glutamic acid-betaxanthin
4-Hydroxycinnamoylagmatine
Epimelibiose
2-Keto-3-Deoxy-D-Mannooctanoic Acid
Ataluren
((2-Amino-3-((2-amino-3-((carboxymethyl)amino)-3-oxopropyl)dithio)propanoyl)amino)acetic acid
2'-Deoxy-2'-fluorocytidine
2-Acetylacteoside
Ajugose
Amylopectin
Maltohexaose
Glucomannan
Cellotetraose
Fumaric acid
Gynocardin
Picolinic acid
IRIDIN
3,7-Dimethylquercetin
Myricanol 5-glucoside
Irigenin
N-gamma-Glutamyl-S-trans-(1-propenyl)cysteine
Prebetanin
LysoPE(16:0/0:0)
Cellopentaose
Lentinan
Pgg-glucan
Gluten exorphin B4
Asparagoside A
Matairesinol
4-Hydroxy-3-methoxycinnamaldehyde
CK2
CK4
CK5
SP_H2
SP_H4
SP_H1
SP_H6
SP_H3
SP_H5
CK1
CK3
CK6
subcluster_1
subcluster_2
subcluster_3
subcluster_4
subcluster_5
subcluster_6
subcluster_7
subcluster_8
subcluster_9
subcluster_10
2
1
0
-1
-2
CK
SP_H

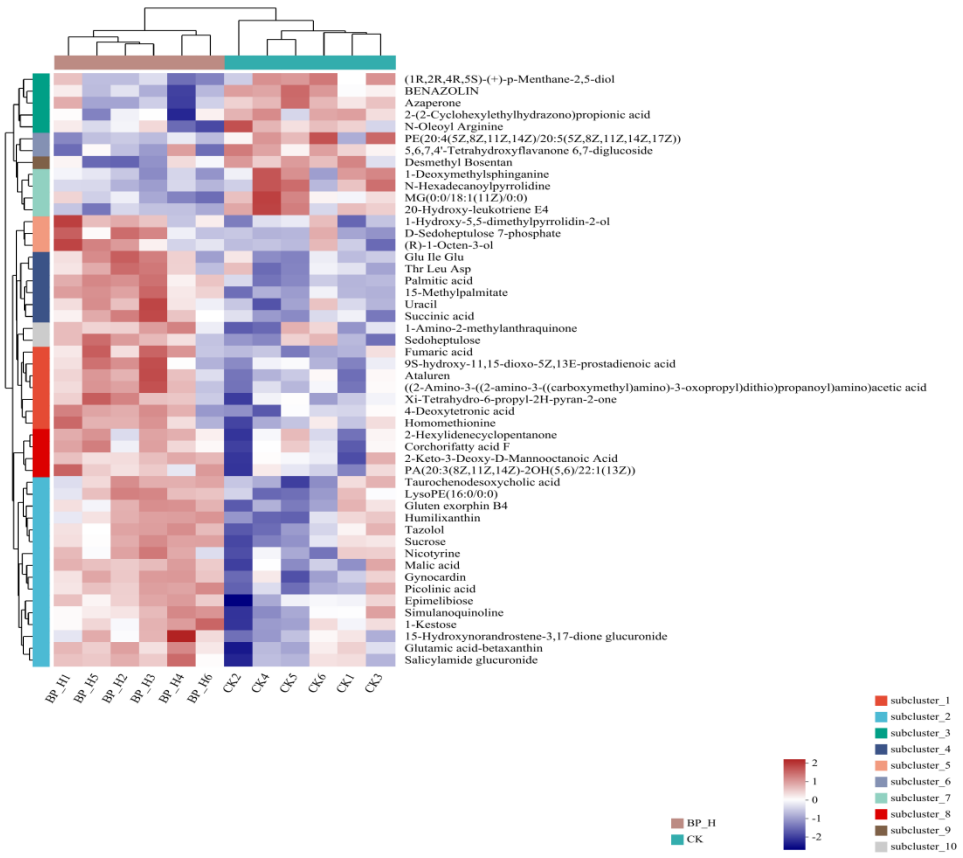
(1R,2R,4R,5S)-(+)-p-Menthane-2,5-diol
BENAZOLIN
Azaperone
2-(2-Cyclohexylethylhydrazono)propionic acid
N-Oleoyl Arginine
PE(20:4(5Z,8Z,11Z,14Z)/20:5(5Z,8Z,11Z,14Z,17Z))
5,6,7,4'-Tetrahydroxyflavanone 6,7-diglucoside
Desmethyl Bosentan
1-Deoxymethylsphinganine
N-Hexadecanoylpyrrolidine
MG(0:0/18:1(11Z)/0:0)
20-Hydroxy-leukotriene E4
1-Hydroxy-5,5-dimethylpyrrolidin-2-ol
D-Sedoheptulose 7-phosphate
(R)-1-Octen-3-ol
Glu Ile Glu
Thr Leu Asp
Palmitic acid
15-Methylpalmitate
Uracil
Succinic acid
1-Amino-2-methylanthraquinone
Sedoheptulose
Fumaric acid
9S-hydroxy-11,15-dioxo-5Z,13E-prostadienoic acid
Ataluren
((2-Amino-3-((2-amino-3-((carboxymethyl)amino)-3-oxopropyl)dithio)propanoyl)amino)acetic acid
Xi-Tetrahydro-6-propyl-2H-pyran-2-one
4-Deoxytetronic acid
Homomethionine
2-Hexylidenecyclopentanone
Corchorifatty acid F
2-Keto-3-Deoxy-D-Mannooctanoic Acid
PA(20:3(8Z,11Z,14Z)-2OH(5,6)/22:1(13Z))
Taurochenodesoxycholic acid
LysoPE(16:0/0:0)
Gluten exorphin B4
Humilixanthin
Tazolol
Sucrose
Nicotyrine
Malic acid
Gynocardin
Picolinic acid
Epimelibiose
Simulanoquinoline
1-Kestose
15-Hydroxynorandrostene-3,17-dione glucuronide
Glutamic acid-betaxanthin
Salicylamide glucuronide
BP_H1
BP_H5
BP_H2
BP_H3
BP_H4
BP_H6
CK2
CK4
CK5
CK6
CK1
CK3
subcluster_1
subcluster_2
subcluster_3
subcluster_4
subcluster_5
subcluster_6
subcluster_7
subcluster_8
subcluster_9
subcluster_10
2
1
0
-1
-2
BP_H
CK

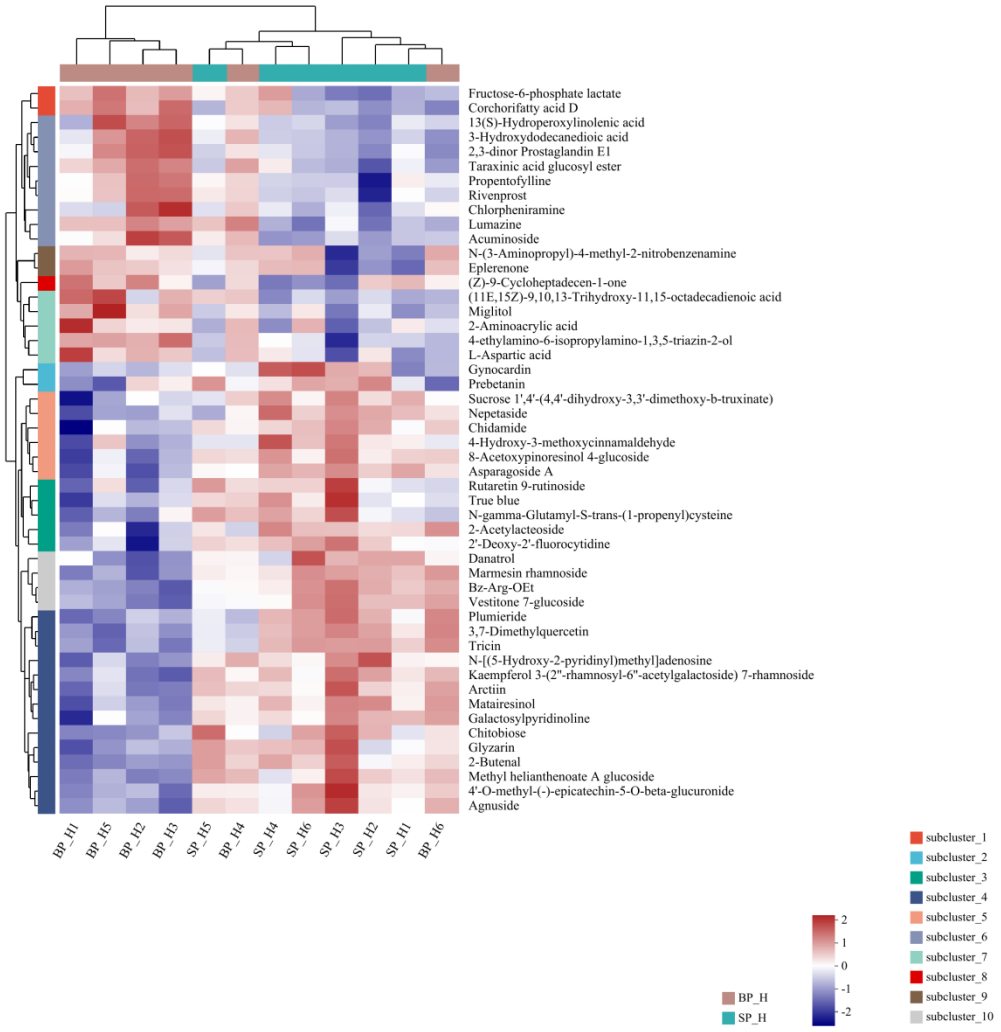

Fig. S3. The clustering heatmaps of three comparison groups.

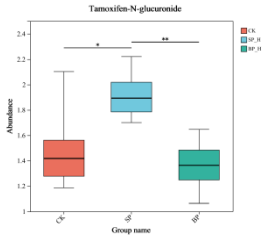
Tamoxifen-N-glucuronide
Abundance
Group name
CK
SP_H
BP_H

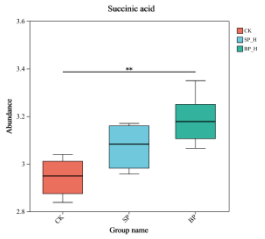
Succinic acid
Abundance
Group name
CK
SP_H
BP_H

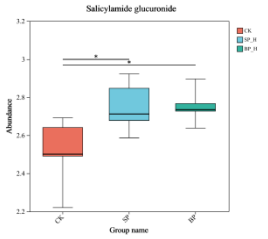
Salicylamide glucuronide
Abundance
Group name
CK
SP_H
BP_H

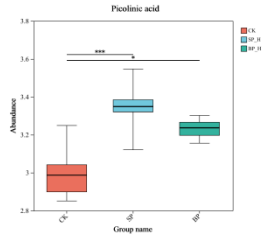
Picolinic acid
Abundance
Group name
CK
SP_H
BP_H

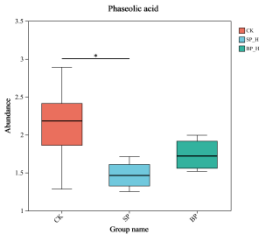
Phaseolic acid
Abundance
Group name
CK
SP_H
BP_H

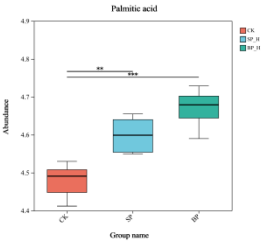
Palmitic acid
Abundance
Group name
CK
SP_H
BP_H

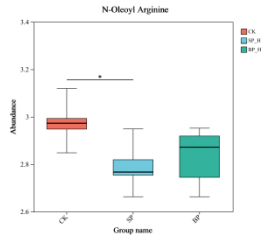
N-Oleoyl Arginine
Abundance
Group name
CK
SP_H
BP_H

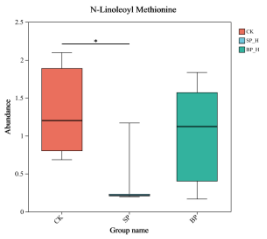
N-Linoleoyl Methionine
Abundance
Group name
CK
SP_H
BP_H

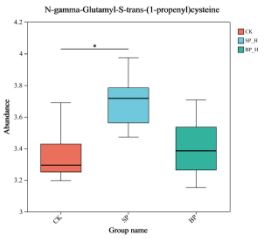
N-gamma-Glutamyl-S-trans-(1-propenyl)cysteine
Abundance
Group name
CK
SP_H
BP_H

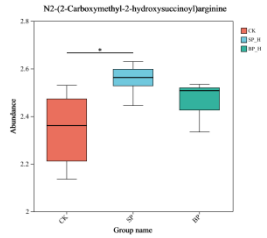
N2-(2-Carboxymethyl-2-hydroxysuccinoyl)arginine
Abundance
Group name
CK
SP_H
BP_H

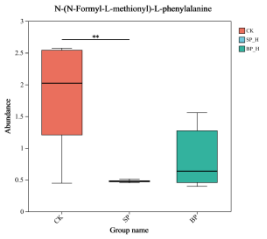
N-(N-Formyl-L-methionyl)-L-phenylalanine
Abundance
Group name
CK
SP_H
BP_H

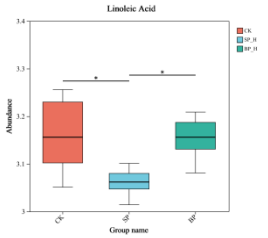
Linoleic Acid
Abundance
Group name
CK
SP_H
BP_H

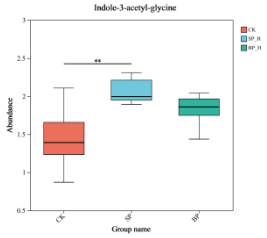
Indole-3-acetyl-glycine
Abundance
Group name
CK
SP_H
BP_H

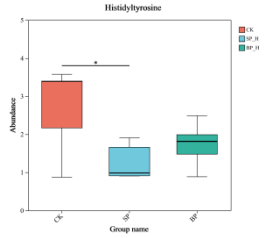
Histidyltyrosine
Abundance
Group name
CK
SP_H
BP_H

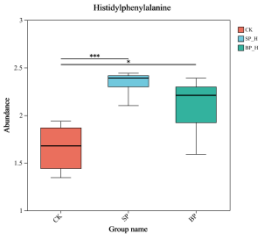
Histidylphenylalanine
Abundance
Group name
CK
SP_H
BP_H

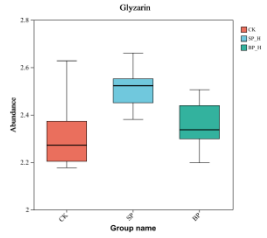
Glyzarin
Abundance
Group name
CK
SP_H
BP_H

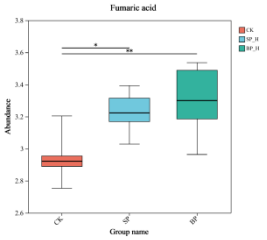
Fumaric acid
Abundance
Group name
CK
SP_H
BP_H

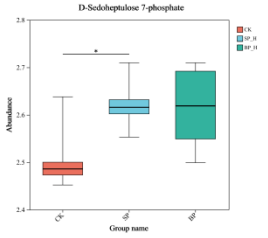
D-Sedoheptulose 7-phosphate
Abundance
Group name
CK
SP_H
BP_H

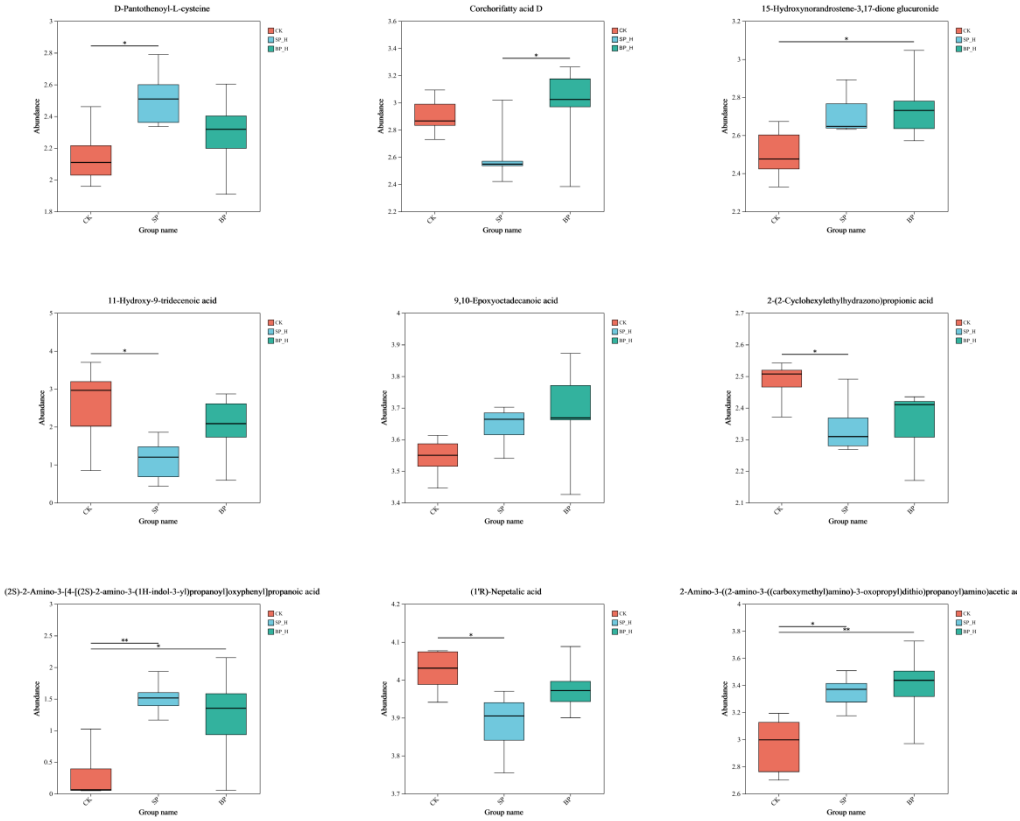

Fig. S4. Effects of triacontanols on LMWOA&AAs metabolism in the SP_H_vs_BP_H_vs_CK comparison group.

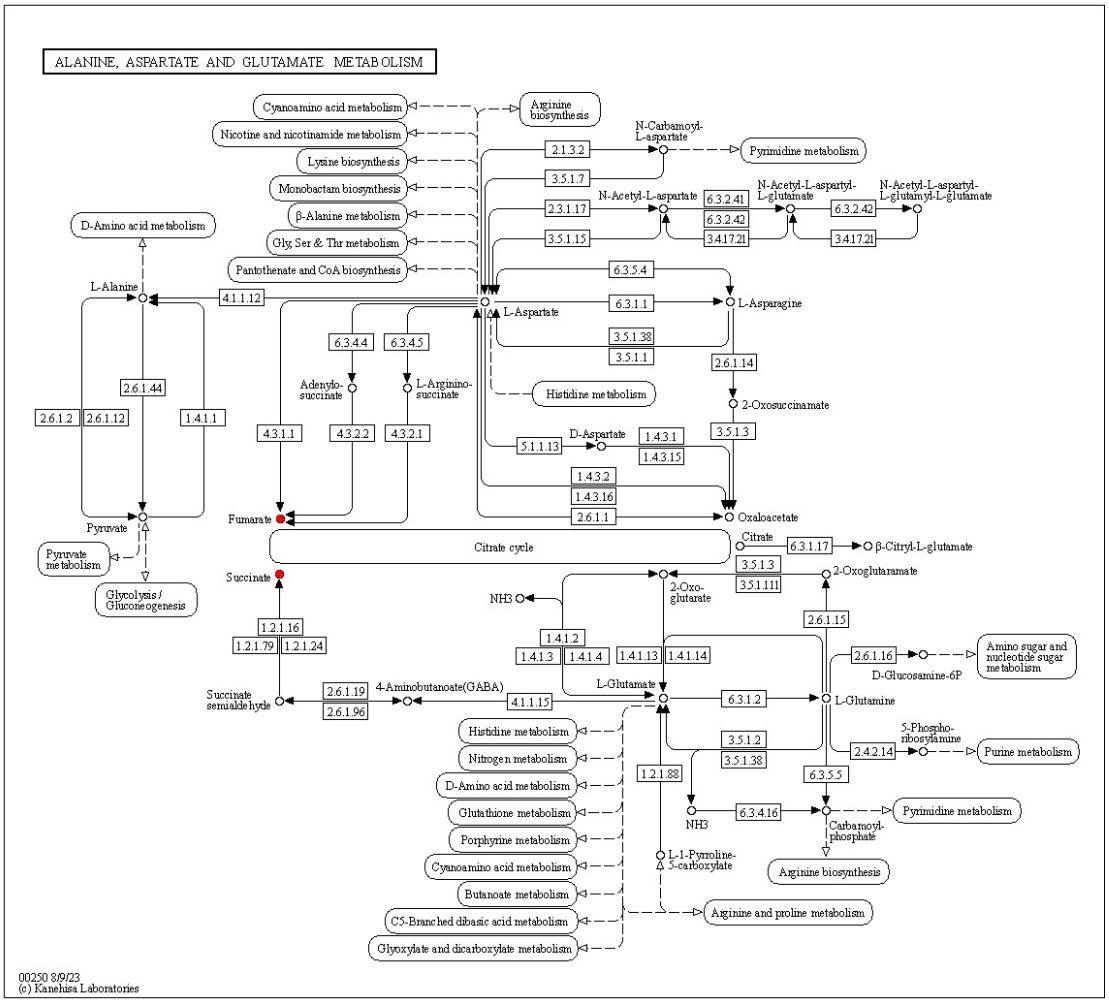

Fig. S5. Alanine, aspartate, and glutamate metabolism pathway (map00250).

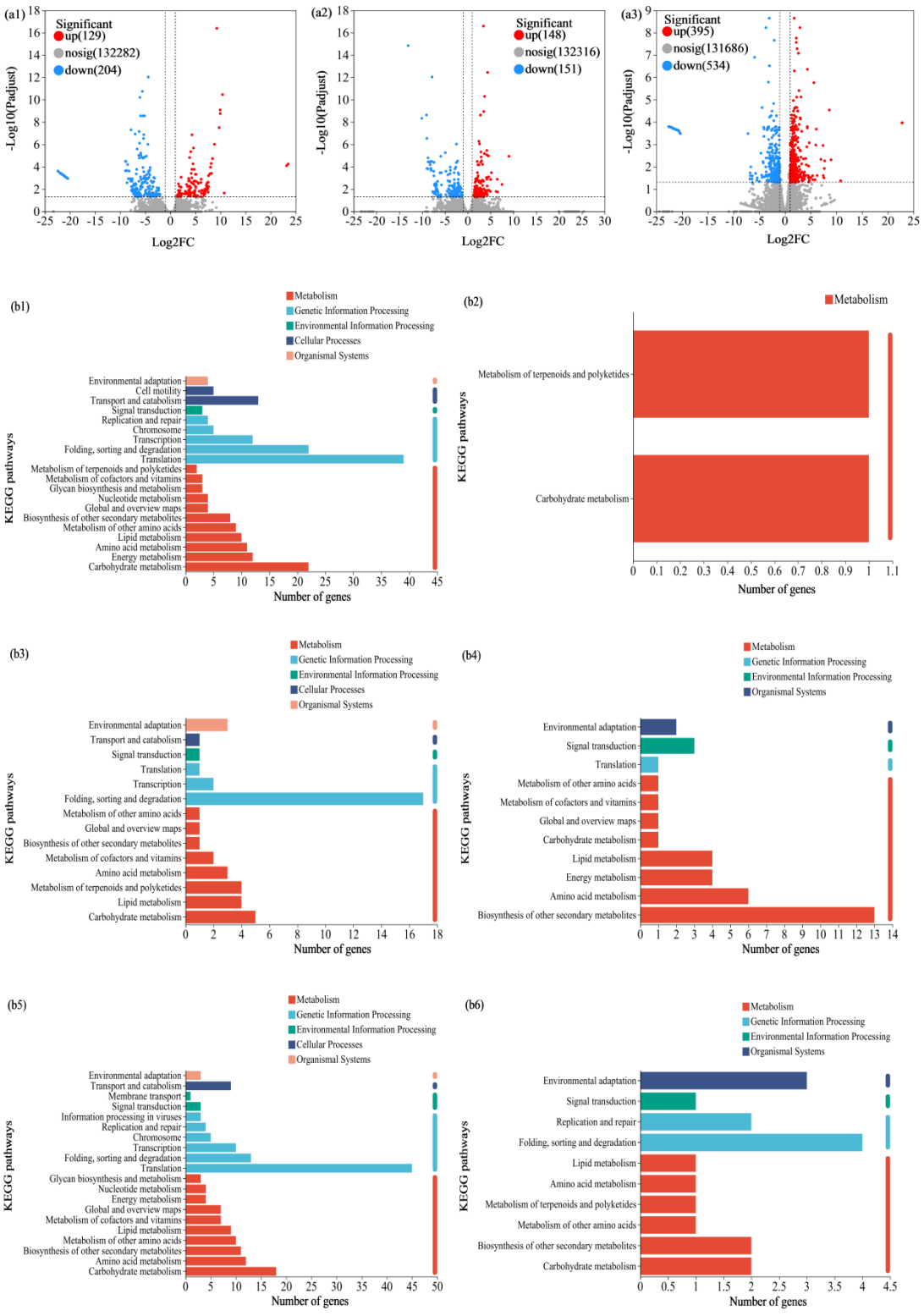

Fig. S6. Effects of triacontanol on gene expression of *T. patula* root. (a) Volcano plots of upregulated and downregulated DEGs in SP_H_vs_CK (a1), BP_H_vs_CK (a2) and SP_H_vs_BP_H (a3); (b) Pathway classification statistics chart for SP_H_vs_CK (b1), BP_H_vs_CK (b2) and SP_H_vs_BP_H (b3).

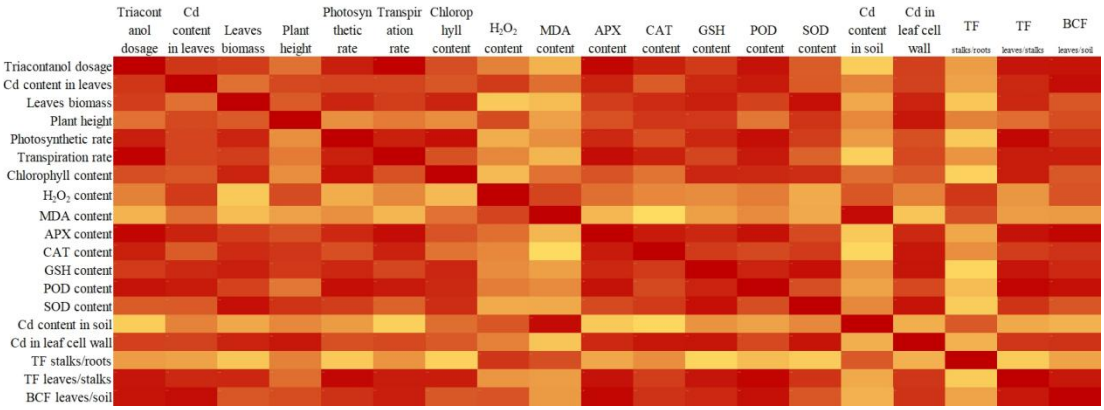

Fig. S7. Pearson correlation analyses of various leaves parameters.

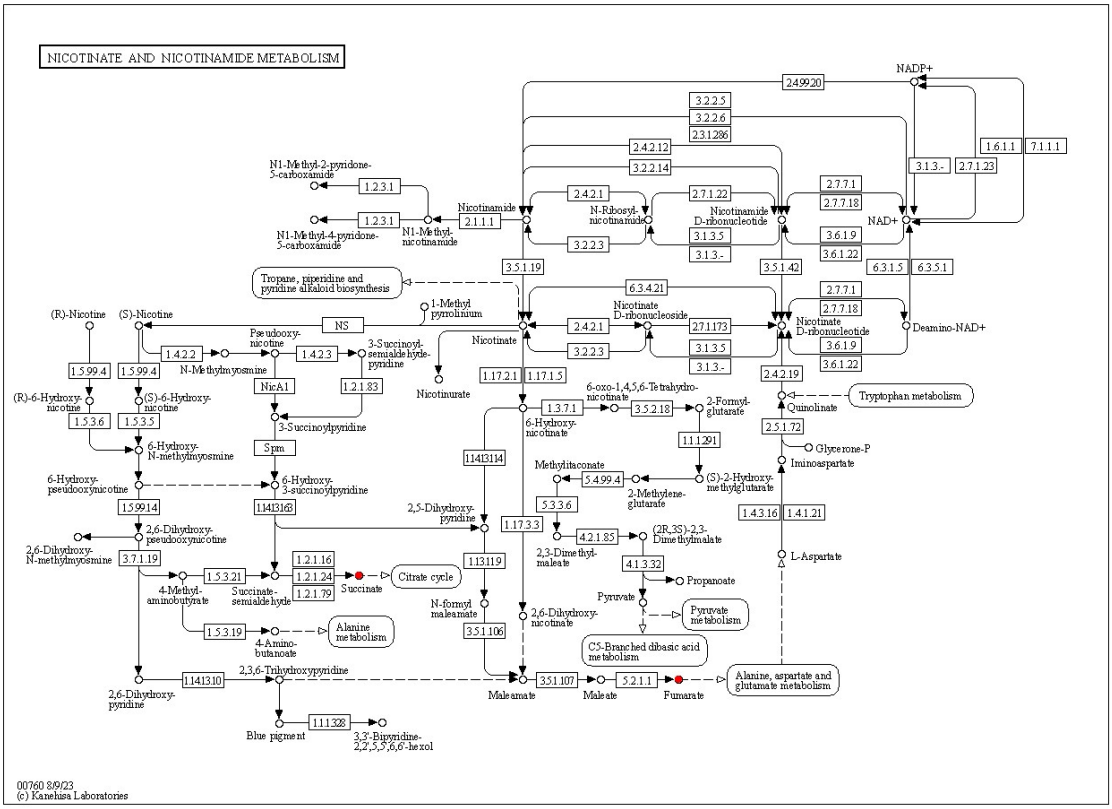

Fig. S8. Nicotinate, and nicotinamide metabolism pathway (map00760).

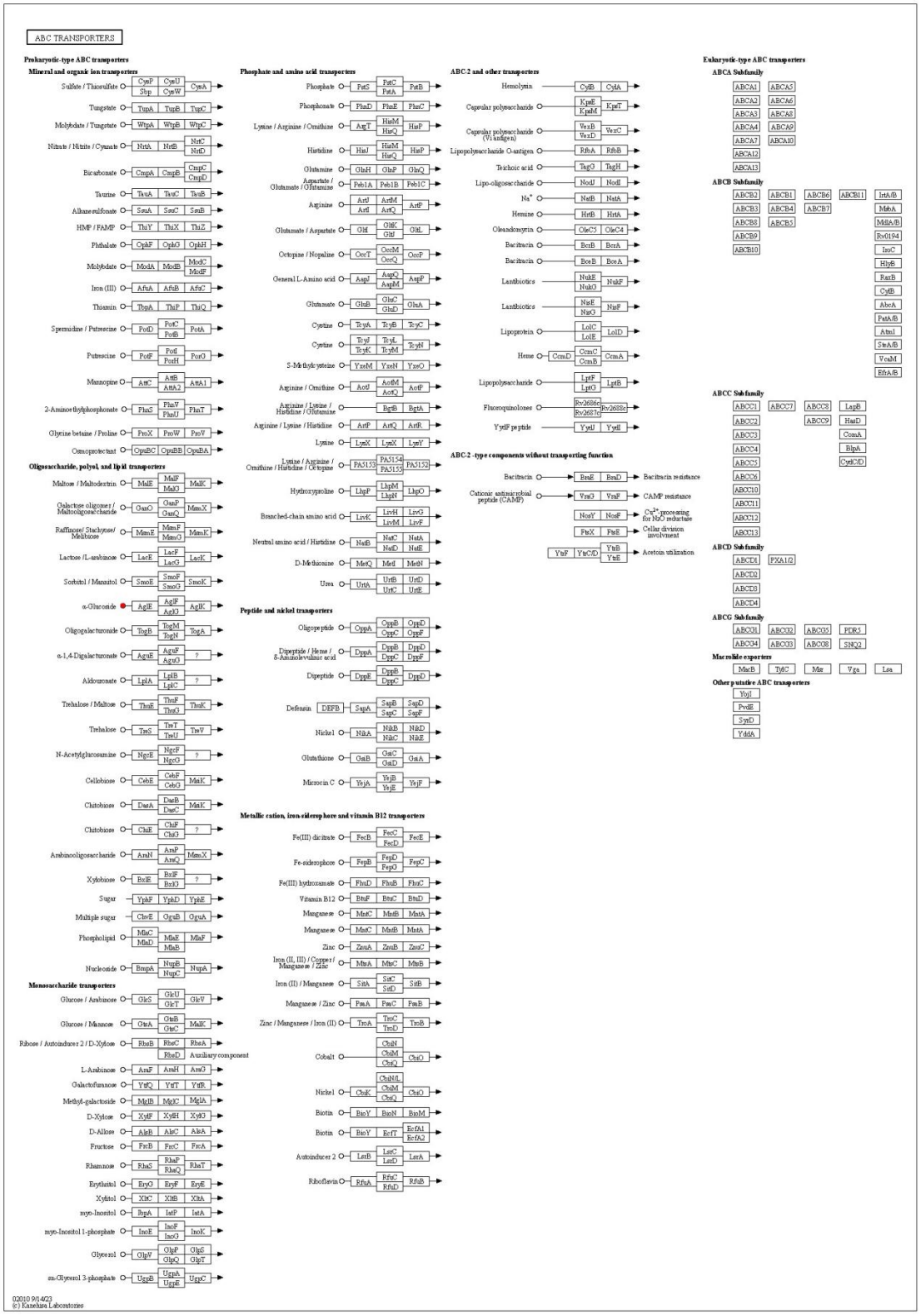

Fig. S9. ABC transporters pathway (map02010).